Timing of Hydrothermal Fluid Flow in the Midcontinent Rift System, Washington County, Kansas

Sahar Mohammadi[1] (sahar@ku.edu), **Andreas Möller**[2] (amoller@ku.edu), **Robert H. Goldstein**[2] (gold@ku.edu)

[1]Kansas Geological Survey, University of Kansas, Lawrence, Kansas, USA
[2]KICE3, Department of Geology, University of Kansas, Lawrence, Kansas, USA

Introduction

The Midcontinent Rift (MCR) in North America is 3,000 km long and resulted from intracontinental rifting, approximately 1.1 billion years ago. The MCR contains a thick succession of basic igneous rocks, predominantly gabbros and basalt (C. A. Stein et al., 2015; S. Stein et al., 2018) and siliciclastic sedimentary rocks. Although primarily resulting from extension, the MCR was structurally inverted after its formation during the Grenville Orogeny (S. Stein et al., 2018).

The MCR comprises two arms: (1) the western arm extends from Minnesota and Iowa to Oklahoma, possibly reaching Texas and New Mexico, based on the occurrence of similar-age diffuse volcanism in those areas (Adams and Keller, 1994, 1996; Bright et al., 2014); (2) the eastern arm stretches southward from Michigan to Alabama, passing through Indiana, Ohio, Kentucky, and Tennessee (Keller et al., 1982; Dickas et al., 1992; C. A. Stein et al., 2014; S. Stein et al., 2018).

The Midcontinent Rift (MCR) is an important geological structure stretching across the Laurentia craton, prominently exposed near Lake Superior with extensive volcanic and sedimentary layers (Ojakangas et al., 2001; Woodruff et al., 2020). Its importance is in explaining why the rift did not lead to the disintegration of Laurentia, possibly due to compressional stresses from the Grenville Orogeny (Hodgin et al., 2022). Consequently, samples from the Jacobsville Formation provide essential geochronological data that can clarify these timing uncertainties, shedding light on the halt of rift development and its connection to regional orogenic processes. Hodgin et al. (2022) used detrital zircon U-Pb geochronology with laser ablation–inductively coupled plasma–mass spectrometry (LA-ICP-MS) to determine the age of the Jacobsville Formation in northern Michigan. They found that the maximum age of this formation is approximately 950 million years old, which is after the Grenville Orogeny, which took place between about 1.09 billion and 980 million years ago (final rift inversion).

In this report, we studied calcite cements in fractures in samples from the Poersch #1 well in Washington County, Kansas (fig. 1) to evaluate the timing of fracturing, fluid composition, and hydrothermal fluid flow as a means of evaluating the early history of the MCR and of determining the timing of presumably Grenville deformation in Kansas.

Geological Background

Berendsen et al. (1988) explored the Midcontinent Rift System in the Kansas Poersch #1 well and reported K/Ar dates of 600–1,000 Ma, which they noted were inconsistent with the timing of rift formation. Van Schmus et al. (1990) and Van Schmus (1992) reported a more reliable U-Pb date of 1,097.5 ± 3 Ma on baddeleyite from a gabbro near the top of the igneous succession in the Poersch #1 well. This date indicated that the basic rocks in the rift in Kansas are time equivalent to the Keweenawan mafic rocks in the northern part of the MCR (Van Schmus, 1992), an indication that the Kansas part of the MCR has a similar origin and timing to that exposed in the Lake Superior region.

According to Berendsen et al. (1988), Paleozoic sediments bury the MCR rocks in Kansas and are typically less than 3,000 ft (900 m) thick. The authors recognized that multiple Phanerozoic phases of deformation could have reactivated structures in the MCR, especially in proximity to the Nemaha tectonic zone, where Ordovician and Carboniferous deformation was recognized (Berendsen et al., 1988).

The research by Berendsen et al. (1988) on the Poersch #1 well in Kansas offered valuable insights into subsurface layers comparable to those exposed in the Lake Superior region. Their study of Precambrian basement rocks was identified in the well at a depth of 2,846 ft (867 m), and drilling reached a total depth of 11,300 ft (3,444 m). The upper portion of the drilled core, down to 7,429 ft (2,264 m), consists predominantly of mafic volcanic rocks and subordinate mafic and acidic intrusions, constituting approximately 90% of the section. The remaining part of the section is dominated by oxidized siltstone, arkose, and sub-arkose.

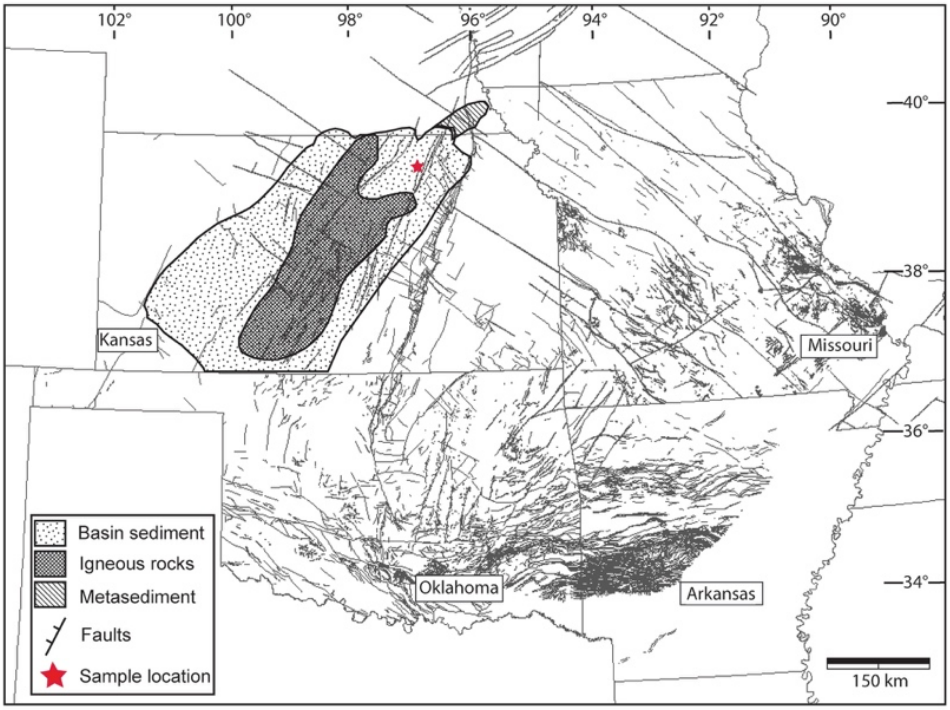

Figure 1. Basement fault map within the present study area, after Bickford et al. (1979), Berendsen et al. (1988), Berendsen and Blair (1991), Northcutt and Campbell (1996), Dicken et al. (2001), USGS (2020), and Mohammadi et al. (2022).

Methods and Results

A. ***Petrography and sample characterization*** **—** Petrographic studies were conducted to define lithology and cement paragenesis. Cold-cathodoluminescence (CL) petrography was carried out using a CITL MK5-1 system mounted on an Olympus-BX53 microscope equipped with 4X, 10X, and 20X long focal distance objective lenses.

Thin section studies show calcite, dolomite, and feldspar filling fractures, vugs, and breccia. These cements were studied with fluid inclusion microthermometry as well as carbon and oxygen isotope and U-Pb analyses to identify their origin and fluid history.

B. ***Fluid inclusion microthermometry*** **—** Fluid inclusion studies were undertaken to determine salinity and temperature of late diagenetic fluids that precipitated the carbonate cements. Fluid inclusion measurements were carried out using a Linkam THMSG 600 heating and cooling stage mounted on an Olympus BX53/60-MTRF-S microscope equipped with 40X and 100X long focal distance objective lenses. This was conducted after full characterization of petrographic associations of fluid inclusions to establish inclusion origin at the level of fluid

inclusion assemblages (FIA; Goldstein and Reynolds, 1994). FIAs are necessary to identify timing of entrapment of fluid inclusions and thermal re-equilibration. Salinities are calculated from T_m measurements using equations of Bodnar (1992). The homogenization temperature (T_h) values ranged from 117°C to 141°C for dolomite cement, from 64°C to 195°C for calcite, and from 91°C to 165°C for feldspar. Additionally, the ice melting temperature (T_m) ranged from -2.2°C to -3.3°C for dolomite, from -0.1°C to -16.5°C for calcite, and from -0.1°C to -22°C for feldspar (wt% NaCl eq.) (table 1).

Table 1. Microthermometric data for dolomite, calcite, and feldspar cements in the Poersch #1 core in Washington County, Kansas. ("Ass." indicates Assemblage).

Sample ID	Mineral	Assemblage	T_h (°C)	T_m (°C)	Description
PO- 5399.92	Calcite	1	63.8	-18.5	Pseudo-secondary
			63.8	-	Pseudo-secondary
			69.8	-17	Pseudo-secondary
			83	-	Pseudo-secondary
			71.7	-	Pseudo-secondary
			83	-	Pseudo-secondary
			-	-11.9	Pseudo-secondary
PO- 5404.17	Feldspar	1			
			-	-0.8	Secondary
			164.8	-0.8	Secondary
			164.8	-0.1	Secondary
			143.6	-0.1	Secondary
			155	-0.1	Secondary
			-	-0.1	Secondary
			136.7	-0.1	Secondary
			136.7	-0.1	Secondary
			136.7	-0.1	Secondary
			147.5	-	Secondary
PO- 7154.83	Dolomite	1			
			125.5	-	Primary
			137.6	-3.3	Primary
			127.7	-2.2	Primary
			127.7	-2.2	Primary
			141	-3.1	Primary
			117	-	Primary
PO- 9164.33	Calcite	1			
		Ass. 1	134	-2.3	Primary

			152	-4.4	Primary
			150	-2.3	Primary
			139.8	-4.4	Primary
		Ass. 2	158.8	-	Primary
			136	-	Primary
			168.7	-2.3	Primary
			-	-3.8	Primary
			158	-	Primary
		Ass. 3	179	-2.3	Primary
			179	-2.3	Primary
			180	-2.3	Primary
		Ass. 4	172	-2.3	Primary
			180	-2.3	Primary
			195	-	Primary
			-	-2.3	Primary
PO- 10515.42	Feldspar	1			
			117	-22	Primary
			91	-22	Primary
			-	-22	Primary
			123.3	-22	Primary
			93.8	-22	Primary
			93.8	-22	Primary
			93.8	-22	Primary
			110	-22	Primary
			-	-22	Primary
			91	-22	Primary
			124.6	-22	Primary
			110	-22	Primary
			110	-22	Primary
			110	-22	Primary
			110	-22	Primary
			91	-22	Primary
			-	-22	Primary
PO- 10659.42	Calcite	1			
			130	-5.2	Primary
			138.6	-7.3	Primary
			133.5	-	Primary
			-	-8.2	Primary
			-	-7.3	Primary
PO- 10662.83	Calcite	1			
			146.1	-3.4	Primary
			141.7	-6.7	Primary
			138.2	-8.5	Primary

			141.7	-9.5	Primary
			140.8	-2.5	Primary
			140.8	-2.5	Primary
			-	-5.7	Primary
			136.8	-2.5	Primary
			136.8	-2.5	Primary
			-	-4.8	
	Calcite	2			
		Ass. 1	144	-12.8	Primary
		Ass. 2	116	-11.3	Primary
		Ass. 3	131.8	-14.4	Primary
			130.2	-13.7	Primary
			130.2	-13.7	Primary
			130.2	-13.7	Primary
			130.2	-13.7	Primary
			131.8	-14.4	Primary
			131.8	-14.4	Primary
			131.8	-13.7	Primary
			131.8	-13.7	Primary
			131.8	-13.7	Primary
			131.8	-13.7	Primary
			131.8	-19.3	Primary
			126.7	-17.3	Primary
			126.7	-17.3	Primary
			126.7	-14.4	Primary
			-	-16.5	
PO- 10651.25	Calcite	1			
		Ass. 1	172	-	Primary
			160	-8.3	Primary
			160	-8.3	Primary
			-	-8.3	Primary
		Ass. 2	155.3	-10.6	Primary
			158.4	-6.2	Primary
		Ass. 3	149.4	-0.1	Primary
			147	-2	Primary
			149	-0.5	Primary
			150	-	Primary
			161	-	Primary
			-	-3.3	Primary
		Ass. 4	144	-8.3	Primary

			152	-8.3	Primary
		Ass. 5	184	-8.3	Primary
			196	-	Primary
		Ass. 6	142.1	-3.3	Primary
			139.5	-3.3	Primary
			142.1	-3.5	Primary
PO- 11291.58	Calcite	1			
		Ass. 1	195.4	-2.1	Primary
		Ass. 2	161	-1.2	Primary
			152.6	-2.3	Primary
			152.6	-4.4	Primary
			151.2	-2.1	Primary
			151.2	-2.1	Primary
		Ass. 3	163	-3.2	Primary
			-	-3.9	Primary

C. Isotope analysis — Carbon and oxygen isotope analyses were conducted on fracture- and vug-filling calcite cements at the Keck-NSF lab at KU. The $\delta^{13}C$ and $\delta^{18}O$ values (relative to the VPDB standard) have standard errors lower than ±0.05‰, based on replicate measurements of the NBS-19 calcite reference standard, and have been corrected for reaction with 100% phosphoric acid at 70°C (Rosenbaum and Sheppard, 1986) (table 2). $^{87}Sr/^{86}Sr$ isotope ratios of late diagenetic calcite cement were determined by thermal ionization mass spectrometry (TIMS) at the University of Kansas Isotope Geochemistry Laboratory (KU-IGL). The values in table 3 have uncertainties of 0.000014 at a 95% confidence interval.

Table 2. Carbon and oxygen isotope data for the Poersch #1 core in Washington County, Kansas.

Sample ID	**Mineral & Open Space Type**	**$\delta^{13}C$ VPDB**	**$\delta^{18}O$ VPDB**
PO-5399.92	vug-filling calcite	-1.82	-14.58
PO-7154.83	breccia-calcite	-3.68	-19.24
PO-9164.33	fracture-filling calcite	-2.16	-23.57
PO-10515.42	fracture-filling calcite	-2.99	-21.22
PO-10659.42	vug-filling calcite	-3.10	-14.27
PO-10662.83	vug-filling calcite	-2.77	-11.95
PO-11291.58	fracture-filling calcite	-3.30	-22.02

Table 3. $^{87}Sr/^{86}Sr$ isotope data for the Poersch #1 core in Washington County, Kansas ("exp corr" refers to exponential correction).

Sample ID	Mineral & Open Space Type	$^{87}Sr/^{86}Sr$ (exp corr)
PO- 5399.92	vug-filling calcite	0.7072776
PO- 9164.33	fracture-filling calcite	0.7133104
PO- 10515	fracture-filling calcite	0.7177937

D. U-Pb dating of carbonate cements and fracture fills **—** Samples were analyzed by LA-ICP-MS to obtain radiometric absolute ages recorded by carbonate growth such as fracture-, breccia-, and vug-filling calcite cements (fig. 2). The method details are described in Gulbranson et al. (2022). Data with high analytical uncertainties (>15% on the isotope ratios, with the exception of absolute uncertainties <0.03 on very low, <0.5 U-Pb ratios) are shown in the diagram but were not used in calculating the discordia arrays and dates. Data with uncertainties >30% on the isotope ratios were not plotted (table 4, fig. 2). For samples 7154.83 and 9164.33, the calculated dates are based on the main data arrays with the lowest intercepts. Data plotting below this array indicate an older age, but poorly defined. Based on the selected data, three of the four samples yield dates between 1,050 ± 53 Ma and 1,108 ± 26 Ma (fig. 2), consistent with the U-Pb baddeleyite age of van Schmus et al. (1990) and early formation of the carbonate cements. All data arrays exhibit excess scatter. Sample 9165 yields an older date of 1,200 ± 54 Ma but is the least radiogenic and is therefore considered the least reliable age estimate for the cements.

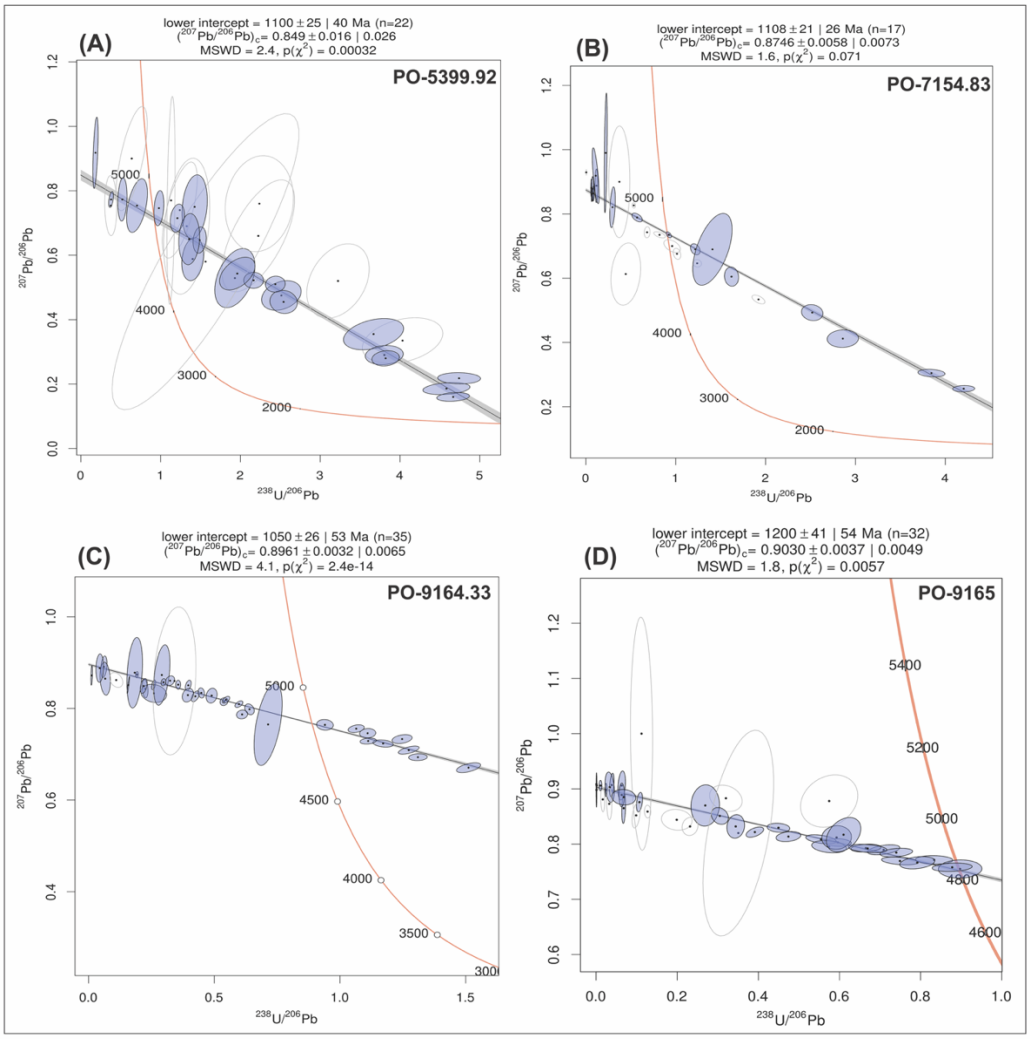

Figure 2. Tera-Wasserburg Concordia diagrams for U-Pb data from calcite cements in samples from the Poersch #1 well in Washington County, Kansas.

Table 4. Supplementary table of U-Pb data from Poersch #1 well in Washington County, Kansas.

Sample from PO-9164.33

No.	^{238}U/ ^{206}Pb*	Prop2SE	^{207}Pb/ ^{206}Pb**	Prop2SE	Rho§	U ppm	±	Th ppm	±	Pb ppm	±
1	0.0123	0.0025	0.8720	0.0170	0.3849	0.002	0.001	b.d.l.		1.058	0.033
2	0.2246	0.0094	0.8430	0.0160	-0.2234	0.052	0.003	b.d.l.		0.919	0.038
3	0.0607	0.0098	0.8910	0.0190	0.2765	0.008	0.002	b.d.l.		0.669	0.022
4	0.0660	0.0164	0.8650	0.0290	-0.1705	0.003	0.001	b.d.l.		0.412	0.023
5	0.2593	0.0410	0.8330	0.0160	-0.1579	0.035	0.005	b.d.l.		0.480	0.025
6	0.5385	0.0127	0.8150	0.0069	0.1411	0.831	0.056	0.005	0.002	5.590	0.320
7	0.4245	0.0130	0.8265	0.0093	0.5086	0.404	0.039	0.001	0.001	3.580	0.320
8	0.2190	0.0113	0.8490	0.0130	0.4051	0.181	0.031	0.002	0.001	3.340	0.660
9	0.4893	0.0175	0.8280	0.0130	0.1723	0.313	0.012	0.005	0.002	2.399	0.078
10	1.1099	0.0258	0.7459	0.0082	0.0772	1.302	0.064	3.400	6.400	4.070	0.180
11	1.2470	0.0321	0.7332	0.0078	0.3235	1.875	0.064	0.207	0.012	5.180	0.120
12§	*0.2717*	*0.1295*	*0.6700*	*0.1000*	*0.0346*	*0.011*	*0.003*	*0.002*	*0.001*	*0.068*	*0.029*

13§	*0.1463*	*0.0563*	*0.9200*	*0.2500*	*0.2729*	*0.009*	*0.006*	*0.600*	*1.200*	*0.270*	*0.150*
14§	*0.1482*	*0.0540*	*1.0600*	*0.4000*	*0.1389*	*0.014*	*0.006*	*2.700*	*5.400*	*0.340*	*0.200*
15	0.5980	0.0126	0.8094	0.0058	0.5307	3.920	0.110	0.239	0.012	23.71	0.690
16	0.6399	0.0151	0.7982	0.0094	-0.2664	3.331	0.048	0.294	0.025	18.88	0.510
17	0.2586	0.0067	0.8517	0.0086	0.4844	0.585	0.010	0.013	0.003	8.740	0.170
18	0.5465	0.0119	0.8190	0.0060	0.5485	4.821	0.049	0.025	0.004	32.66	0.390
19	1.0644	0.0256	0.7558	0.0068	0.3168	8.960	0.310	0.123	0.006	28.29	0.770
20	0.9399	0.0268	0.7642	0.0093	-0.0684	6.230	0.330	0.115	0.011	22.12	0.750
21	0.3563	0.0078	0.8519	0.0078	0.0129	3.143	0.039	0.221	0.017	33.89	0.430
22	0.3963	0.0094	0.8505	0.0090	0.4308	3.045	0.075	0.108	0.018	29.16	0.580
23	0.1923	0.0044	0.8739	0.0056	0.1511	4.239	0.034	0.004	0.001	86.90	1.200
24	0.2911	0.0258	0.8730	0.0530	0.4057	0.097	0.016	b.d.l.		1.530	0.390
25	0.1834	0.0250	0.8780	0.0620	0.2757	0.014	0.002	b.d.l.		0.281	0.050
26§	*0.3169*	*0.2026*	*0.8200*	*0.3000*	*-0.0045*	*0.008*	*0.005*	*0.002*	*0.003*	*0.064*	*0.052*
27§	*0.1028*	*0.0288*	*1.3500*	*0.4300*	*0.2655*	*0.013*	*0.005*	*0.001*	*0.001*	*0.210*	*0.120*
28§	*0.0679*	*0.0328*	*0.8400*	*0.3000*	*0.5590*	*0.010*	*0.005*	*0.060*	*0.11*	*0.230*	*0.120*
29§	*0.0761*	*0.0659*	*0.5100*	*0.1800*	*0.8587*	*0.001*	*0.001*	*0.450*	*0.63*	*0.027*	*0.013*
30	0.3948	0.0180	0.8290	0.0120	0.2504	0.123	0.010	0.002	0.001	1.200	0.082
31	1.1715	0.0327	0.7235	0.0063	-0.2703	4.122	0.041	0.069	0.005	11.32	0.220
32	1.1121	0.0259	0.7289	0.0053	0.2150	5.151	0.048	0.237	0.008	15.04	0.200
33	1.2734	0.0331	0.7090	0.0071	0.6088	4.873	0.086	0.206	0.015	12.03	0.280
34	1.3100	0.0298	0.6936	0.0059	0.0828	6.831	0.066	0.598	0.05	16.33	0.270
35	1.5113	0.0386	0.6707	0.0086	0.5488	7.077	0.078	0.394	0.019	13.95	0.240
36§	*0.2153*	*0.1219*	*0.6700*	*0.2100*	*-0.0174*	*0.009*	*0.008*	*0.001*	*0.002*	*0.160*	*0.110*
37	*0.1097*	*0.0212*	*0.8620*	*0.0130*	*-0.3054*	*0.015*	*0.004*	*0.001*	*0.001*	*0.607*	*0.023*
38	0.4482	0.0102	0.8339	0.0089	-0.1603	1.772	0.030	0.326	0.014	14.71	0.240
39	0.3241	0.0143	0.8606	0.0085	0.2306	0.221	0.011	b.d.l.		2.770	0.140
40	0.1580	0.0040	0.8510	0.0150	0.8971	0.157	0.003	0.236	0.015	4.040	0.180
41	0.0442	0.0120	0.8880	0.0250	0.0981	0.003	0.001	b.d.l.		0.512	0.019
42	0.6105	0.0179	0.7870	0.0078	0.1156	0.470	0.016	0.033	0.015	2.680	0.110
43	0.7140	0.0450	0.7650	0.0720	0.5001	1.300	0.110	0.186	0.028	6.110	0.850
44	0.2975	0.0076	0.8572	0.0063	0.1985	0.851	0.014	10.00	15.00	10.90	0.230
45	*0.3416*	*0.0688*	*0.8600*	*0.1300*	*0.1961*	*0.008*	*0.001*	*0.003*	*0.002*	*0.087*	*0.023*

PO-7154.83

No.	$^{238}U/^{206}Pb^*$	2SE abs	$^{207}Pb/^{206}Pb$	2SE abs	Rhoζ	U ppm	±	Th ppm	±	Pb ppm	±
1	0.9231	0.0235	0.7350	0.0075	-0.5470	1.990	0.091	2.770	0.790	7.440	0.210
2	*0.6816*	*0.0262*	*0.7430*	*0.0140*	*0.0863*	*0.485*	*0.017*	*3.820*	*0.220*	*2.674*	*0.077*
3	*1.0142*	*0.0339*	*0.6760*	*0.0140*	*-0.2620*	*0.670*	*0.04*	*1.870*	*0.280*	*2.190*	*0.160*
4	*1.9209*	*0.0580*	*0.5340*	*0.0110*	*-0.5694*	*1.514*	*0.041*	*2.350*	*0.240*	*2.070*	*0.120*
5	*0.8197*	*0.0518*	*0.7351*	*0.0079*	*-0.5857*	*0.602*	*0.072*	*1.600*	*0.150*	*2.480*	*0.160*
6	1.2177	0.0430	0.6900	0.0140	-0.3135	0.496	0.019	0.924	0.064	1.329	0.068
7	*1.2389*	*0.0388*	*0.6464*	*0.0094*	*-0.0810*	*0.297*	*0.03*	*0.428*	*0.086*	*0.739*	*0.064*
8	0.2207	0.0127	0.9900	0.1500	0.4838	0.001	<0.001	0.004	0.001	0.032	0.004
9§	*0.1375*	*0.0696*	*0.7900*	*0.2200*	*0.9983*	*0.001*	*<0.001*	*0.010*	*0.002*	*0.031*	*0.004*
10	0.1176	0.0135	0.8880	0.0420	0.0357	0.003	<0.001	0.044	0.003	0.102	0.007
11	0.1097	0.0307	0.9190	0.0700	-0.7103	0.002	0.001	0.129	0.006	0.098	0.006
12	1.4086	0.1759	0.6900	0.0900	0.5492	0.006	<0.001	0.066	0.007	0.017	0.003
13	0.2964	0.0245	0.8210	0.0510	0.3844	0.006	0.001	0.066	0.006	0.074	0.009
14	*0.3729*	*0.0941*	*0.9000*	*0.1400*	*0.0132*	*0.057*	*0.012*	*8.500*	*7.600*	*0.370*	*0.150*
15	1.6207	0.0632	0.6050	0.0240	-0.0756	0.098	0.003	b.d.l.		0.163	0.010
16	2.5188	0.0960	0.4930	0.0200	-0.1166	0.110	0.003	0.001	0.001	0.097	0.008
17	0.0613	0.0060	0.8810	0.0220	0.1795	0.003	<0.001	0.029	0.003	0.173	0.009
18	*0.9604*	*0.0742*	*0.7000*	*0.0160*	*-0.4746*	*0.116*	*0.013*	*0.040*	*0.007*	*0.350*	*0.021*
19	2.8597	0.1399	0.4120	0.0220	0.0514	0.093	0.001	0.098	0.007	0.055	0.006
20	0.5332	0.0153	0.8266	0.0068	-0.0933	1.346	0.044	1.860	0.380	9.660	0.300
21	*0.0040*	*0.0009*	*0.9295*	*0.0073*	*-0.0852*	*0.029*	*0.009*	*0.061*	*0.014*	*14.78*	*0.69*
22	0.0761	0.0097	0.8780	0.0310	-0.0794	0.005	0.001	b.d.l.		0.268	0.016
23	*0.4440*	*0.1333*	*0.6130*	*0.0780*	*0.1843*	*0.045*	*0.015*	*2.800*	*4.000*	*0.270*	*0.190*
24	0.0656	0.0043	0.8620	0.0190	0.0850	0.005	<0.001	0.021	0.011	0.290	0.033

25	3.8457	0.1213	0.3048	0.0096	-0.2046	1.083	0.041	0.129	0.012	0.316	0.013
26	4.2041	0.0988	0.2563	0.0079	0.0560	0.713	0.010	0.122	0.005	0.159	0.007
27	0.0845	0.0071	0.8640	0.0190	0.2696	0.006	<0.001	0.021	0.002	0.294	0.017
28	0.5705	0.0469	0.7890	0.0110	-0.5436	0.215	0.022	1.380	0.260	1.419	0.036

PO-5399.92

No.	$^{238}U/^{206}Pb^{*}$	2SE abs	$^{207}Pb/^{206}Pb^{**}$	2SEabs	Rhoʒ	U ppm	±	Th ppm	±	Pb ppm	±
1§	*1.1308*	*0.0408*	*0.7700*	*0.2600*	*0.3302*	*0.002*	*<0.001*	*b.d.l.*		*0.007*	*0.001*
2	0.7043	0.1052	0.7540	0.0670	0.4672	0.003	<0.001	b.d.l.		0.015	0.003
3	0.3791	0.0238	0.7730	0.0200	0.4808	0.006	<0.001	b.d.l.		0.063	0.007
4	*2.2242*	*0.3666*	*0.6600*	*0.1400*	*0.6373*	*0.003*	*<0.001*	*b.d.l.*		*0.005*	*0.001*
5	*1.3268*	*0.2328*	*0.6900*	*0.1700*	*0.2758*	*0.003*	*<0.001*	*b.d.l.*		*0.005*	*0.002*
6	1.9306	0.2026	0.5290	0.0740	0.4078	0.004	<0.001	b.d.l.		0.007	0.001
7§	*1.5630*	*0.9426*	*0.5800*	*0.3700*	*0.8614*	*0.001*	*<0.001*	*b.d.l.*		*0.006*	*0.001*
8	1.4017	0.1100	0.5880	0.0540	0.1943	0.004	<0.001	b.d.l.		0.007	0.001
9	0.1834	0.0262	0.9180	0.0890	0.5202	0.002	<0.001	b.d.l.		0.040	0.004
10	*0.6374*	*0.1571*	*0.9000*	*0.1300*	*0.6727*	*0.002*	*<0.001*	*b.d.l.*		*0.009*	*0.001*
11	*4.0318*	*0.4061*	*0.3350*	*0.0570*	*0.3140*	*0.010*	*<0.001*	*b.d.l.*		*0.004*	*0.001*
12	0.5210	0.0463	0.7730	0.0540	0.1575	0.004	<0.001	b.d.l.		0.021	0.003
13	*3.2232*	*0.3155*	*0.5200*	*0.0930*	*0.3270*	*0.005*	*<0.001*	*b.d.l.*		*0.004*	*0.001*
14	*2.2373*	*0.3448*	*0.7600*	*0.1200*	*0.1111*	*0.005*	*<0.001*	*b.d.l.*		*0.008*	*0.002*
15	*1.2402*	*0.1768*	*0.7400*	*0.1200*	*0.6497*	*0.003*	*<0.001*	*b.d.l.*		*0.009*	*0.002*
16	2.5132	0.1995	0.4750	0.0370	0.2828	0.015	0.001	b.d.l.		0.015	0.002
17	3.6688	0.3030	0.3550	0.0390	0.3564	0.018	0.001	b.d.l.		0.007	0.001
18	*0.3753*	*0.0609*	*0.7540*	*0.0750*	*-0.0605*	*0.002*	*<0.001*	*b.d.l.*		*0.021*	*0.002*
19	2.5412	0.1387	0.4550	0.0290	-0.0757	0.032	0.003	b.d.l.		0.027	0.002
20	4.5824	0.2372	0.1860	0.0150	0.2660	0.082	0.006	b.d.l.		0.010	0.002
21	4.6667	0.1649	0.1600	0.0110	0.2153	0.099	0.005	b.d.l.		0.009	0.001
22	1.4263	0.1277	0.7500	0.0800	0.2055	0.015	0.001	b.d.l.		0.036	0.004
23	2.1651	0.0992	0.5220	0.0200	0.0075	0.057	0.003	b.d.l.		0.060	0.004
24	3.8034	0.1915	0.2900	0.0240	0.1108	0.057	0.002	b.d.l.		0.019	0.002
25	2.4380	0.0998	0.5100	0.0200	0.0512	0.052	0.004	b.d.l.		0.043	0.004
26	1.4896	0.0665	0.6470	0.0330	0.1690	0.018	0.001	b.d.l.		0.038	0.003
27	0.9786	0.0497	0.7460	0.0440	0.2433	0.023	0.001	b.d.l.		0.080	0.005
28	1.2100	0.0717	0.7150	0.0350	0.2392	0.013	0.001	b.d.l.		0.034	0.003
29	1.9605	0.1790	0.5430	0.0410	0.4572	0.036	0.005	b.d.l.		0.039	0.003
30	1.3583	0.1051	0.6500	0.0640	0.1070	0.016	0.002	b.d.l.		0.035	0.005
31	4.7404	0.2163	0.2180	0.0140	-0.0549	0.292	0.025	b.d.l.		0.045	0.005
32	3.8199	0.1391	0.2800	0.0190	0.1459	0.105	0.007	b.d.l.		0.027	0.003

PO- 9165

	$^{238}U/^{206}Pb^{*}$	2SE abs	$^{207}Pb/^{206}Pb^{**}$	2SEabs	Rhoʒ	U ppm	±	Th ppm	±	Pb ppm	±
1	0.02439	0.00203	0.8980	0.0097	0.0684	0.007	0.001	b.d.l.		1.130	0.040
2	0.06795	0.00373	0.8650	0.0221	0.2400	0.013	<0.001	b.d.l.		0.705	0.020
3	0.44959	0.02243	0.8296	0.0066	-0.1599	3.279	0.049	0.001	0.001	25.55	0.650
4	0.06307	0.0075	0.9060	0.0212	0.2414	0.009	0.001	b.d.l.		0.523	0.024
5	0.03864	0.00451	0.9070	0.0172	0.3719	0.006	0.001	b.d.l.		0.577	0.020
6	0.39138	0.01734	0.8217	0.0075	0.5407	0.369	0.038	b.d.l.		3.280	0.330
7	*0.01638*	*0.00394*	*0.8810*	*0.0182*	*-0.1219*	*0.001*	*<0.001*	*b.d.l.*		*0.662*	*0.020*
8	0.59579	0.02669	0.8029	0.0057	-0.1265	5.220	0.120	0.005	0.001	29.67	0.330
9	0.70894	0.03201	0.7897	0.0073	0.4307	4.697	0.083	0.014	0.003	22.55	0.600
10	0.55454	0.03026	0.8087	0.0066	-0.4443	3.696	0.098	0.001	0.001	22.48	0.360
11	*0.57458*	*0.05685*	*0.8780*	*0.0381*	*0.2103*	*0.279*	*0.037*	*b.d.l.*		*1.880*	*0.150*
12	*0.31995*	*0.03226*	*0.8830*	*0.0192*	*-0.2224*	*0.109*	*0.011*	*b.d.l.*		*1.290*	*0.067*
13	0.74911	0.03648	0.7695	0.0057	-0.3337	1.701	0.061	b.d.l.		7.330	0.130
14	*0.19881*	*0.03049*	*0.8440*	*0.0152*	*-0.0962*	*0.041*	*0.006*	*b.d.l.*		*0.655*	*0.026*
15	0.03356	0.00919	0.9030	0.0221	-0.2567	0.002	0.001	b.d.l.		0.420	0.013
16	0.66511	0.02990	0.7928	0.0057	0.2079	4.060	0.043	0.018	0.002	20.67	0.340
17	0.26898	0.02822	0.8700	0.0301	0.0447	0.052	0.008	b.d.l.		0.711	0.061

18	0.10686	0.00612	0.8760	0.0142	0.3678	0.043	0.005	b.d.l.		1.480	0.120
19	*0.12687*	*0.00629*	*0.8589*	*0.0093*	*-0.0478*	*0.046*	*0.002*	*b.d.l.*		*1.329*	*0.069*
20	0.74001	0.03238	0.7846	0.0064	0.3020	5.204	0.040	0.002	0.001	23.75	0.410
21	0.83329	0.03704	0.7714	0.0062	-0.0723	2.215	0.087	b.d.l.		8.740	0.460
22	0.79180	0.03467	0.7663	0.0090	0.2972	0.735	0.012	b.d.l.		3.016	0.053
23	0.57427	0.03443	0.7954	0.0089	-0.2384	0.322	0.011	b.d.l.		1.849	0.032
24	0.06307	0.00542	0.8890	0.0172	0.0465	0.011	0.001	b.d.l.		0.667	0.023
25	0.47406	0.02448	0.8136	0.0073	0.2566	0.280	0.009	b.d.l.		1.999	0.068
26	0.66958	0.03842	0.7921	0.0061	-0.3449	3.820	0.150	0.004	0.001	18.87	0.220
27	0.59289	0.02944	0.8120	0.0172	0.0496	0.665	0.008	b.d.l.		3.760	0.230
28	0.30484	0.01708	0.8510	0.0122	-0.2188	0.392	0.023	b.d.l.		4.610	0.140
29	*0.35062*	*0.07025*	*0.8200*	*0.1500*	*0.4842*	*0.054*	*0.015*	*0.003*	*0.003*	*0.460*	*0.210*
30	0.61003	0.03420	0.8170	0.0251	0.3562	0.478	0.026	0.010	0.006	2.900	0.480
31	0.89733	0.04326	0.7550	0.0132	0.0336	0.608	0.023	0.001	0.001	2.107	0.063
32	*0.11198*	*0.02197*	*1.0000*	*0.1700*	*-0.0626*	*0.037*	*0.014*	*0.600*	*1.200*	*1.380*	*0.580*
33	0.87795	0.03964	0.7580	0.0061	0.1875	1.872	0.028	0.031	0.051	6.800	0.140
34	0.34424	0.01746	0.8320	0.0172	0.1008	0.081	0.003	b.d.l.		0.824	0.021
35	*0.09860*	*0.00810*	*0.8520*	*0.0182*	*0.3915*	*0.022*	*0.002*	*b.d.l.*	*0.05*	*0.823*	*0.051*
36	*0.23153*	*0.01579*	*0.8320*	*0.0132*	*0.0856*	*0.051*	*0.002*	*b.d.l.*	*0.05*	*0.714*	*0.019*
37	*0.03228*	*0.00503*	*0.8730*	*0.0231*	*-0.1039*	*0.008*	*0.001*	*b.d.l.*	*0.05*	*0.855*	*0.050*
38	0.00096	0.00064	0.8980	0.0251	0.0277	0.001	<0.001	b.d.l.		13.22	0.470
39	0.00073	0.00009	0.9086	0.0083	-0.0996	0.002	<0.001	b.d.l.		11.40	0.690
40	0.00139	0.00039	0.9060	0.0142	-0.0487	0.002	<0.001	0.005	0.003	10.95	0.300
41	0.01076	0.00276	0.9060	0.0076	0.0348	0.018	0.003	b.d.l.		6.040	0.200
42	0.06816	0.02380	0.8850	0.0113	-0.0870	0.056	0.019	b.d.l.		2.093	0.066
43	0.02439	0.00203	0.9090	0.0123	-0.4015	0.003	0.004	b.d.l.	0.05	18.07	0.230

Footnotes:
Italics: data omitted from calculations, as described in the main text.
§: omitted from calculations and not plotted due to uncertainty >30%.
*: ratio corrected for elemental fractionation, based on reference material DBTL, in addition to corrections for **.
**: ratio corrected for laser-induced fractionation and drift, based on reference material NIST 612.
ʒ: error correlation
b.d.l.: below detection limit (detection limit estimated to be 1 ppb). Data reported to single ppb.

References

Adams, D. C., and Keller, G. R., 1994, Possible extension of the Midcontinent Rift in West Texas and eastern New Mexico: Canadian Journal of Earth Sciences, v. 31, n. 4, p. 709–720.

Adams, D. C., and Keller, G. R., 1996, Precambrian basement geology of the Permian Basin region of West Texas and eastern New Mexico: a geophysical perspective: AAPG Bulletin, v. 80, n. 3, p. 410–431.

Berendsen, P., and Blair, K. P., 1991, Interpretive subcrop map of the Precambrian basement in the Joplin 10 x 20 quadrangle: Kansas Geological Survey, Subsurface Geology Series 14, 10 p.

Berendsen, P., Borcherding, R. M., Doveton, J., Gerhard, L., Newell, K. D., Steeples, D., and Watney, W. L., 1988, Texaco Poersch #1, Washington County, Kansas—Preliminary

geologic report of the pre-Phanerozoic rocks: Kansas Geological Survey, Open-File Report 88-22.

Bickford, M. E., Richard, D. L., 1979, U-Pb geochronology of exposed basement rocks in Oklahoma: GSA Bulletin, v. 90, no. 6, p. 540–544. doi: https://doi.org/10.1130/0016-7606(1979)90<540:UGOEBR>2.0.CO;2

Bodnar, R. J., 1992, Revised equation and table for determining the freezing point depression of H_2O-NaCl solutions: Geochimica et Cosmochimica Acta, v. 57, p. 683–684.

Bright, R. M., Amato, J. M., Denyszyn, S. W., and Ernst, R. E., 2014, U-Pb geochronology of 1.1 Ga diabase in the southwestern United States: testing models for the origin of a post-Grenville large igneous province: Lithosphere, v. 6, p. 135–156.

Dickas, A. B., Mudrey, M. G., Ojakangas, R. W., and Shranke, D. L., 1992, A possible southeastern extension of the Midcontinent rift system located in Ohio: Tectonics, v. 11, p. 1,406–1,414, doi:10.1029 /91TC02903.

Dicken, C. L., Pimley, S. G., and Cannon, W. F., 2001, Precambrian basement map of the northern midcontinent, U.S.A. — A digital representation of the 1990 P. K. Sims map: U.S. Geological Survey Open-File Report 01-021, available online only.

Goldstein, R. H., and Reynolds, T. J., 1994, Systematics of fluid inclusions in diagenetic minerals: Society for Sedimentary Geology (SEPM) short course 31, 199 p.

Gulbranson, E. L., Rasbury, E. T., Ludvigson, G. A., Möller, A., Henkes, G. A., Suarez, M. B., Northrup, P., Tappero, R. V., Maxson, J. A., Shapiro, R. S. and Wooton, K. M., 2022, U–Pb geochronology and stable isotope geochemistry of terrestrial carbonates, Lower Cretaceous Cedar Mountain Formation, Utah: Implications for synchronicity of terrestrial and marine carbon isotope excursions: Geosciences, v. 12, no. 9, p. 346, doi:10.3390/geosciences12090346.

Hodgin, E. B., Swanson-Hysell, N. L., DeGraff, J. M., Kylander-Clark, A. R. C., Schmitz, M. D., Turner, A. C., Zhang, Y., and Stolper, D. A., 2022, Final inversion of the Midcontinent Rift during the Rigolet Phase of the Grenvillian orogeny: Geology, doi:10.1130/G49439.1.

Keller, G. R., Bland, A. E., and Greenberg, J. K., 1982, Evidence for a major Late Precambrian tectonic event (rifting?) in the eastern midcontinent region, United States: Tectonics, v. 1, p. 213–223, doi: 10 .1029 /TC001i002p00213.

Mohammadi, S., Hollenbach, A., Goldstein, R. H., Möller, A., Burberry, C. M., 2022, Controls on timing of hydrothermal fluid flow in south-central Kansas, north-central Oklahoma, and the Tri-State Mineral District: Midcontinent Geoscience, v. 3, p. 1–26.

Northcutt, R. A., and Campbell, J. A., 1996, Geologic provinces of Oklahoma: The Shale Shaker, v. 46, p. 99–103.

Ojakangas, R. W., Morey, G. B., and Green, E. C., 2001, The Mesoproterozoic midcontinent rift system, Lake Superior region, USA: Sedimentary Geology, v. 141, p. 421–442.

Rosenbaum, J., and Sheppard, S. M. F., 1986, An isotopic study of siderites, dolomites and ankerites at high temperatures: Geochimica et Cosmochimica Acta, v. 50, p. 1,147–1,150.

Stein, C. A., Kley, J., Stein, S., Hindle, D., and Keller, G. R., 2015, North America's Midcontinent Rift: When rift met LIP: Geosphere, v. 11, n. 5, p. 1,607–1,616, doi:10.1130/GES01183.1

Stein, C. A., Stein, S., Merino, M., Keller, G. R., Flesch, L. M., and Jurdy, D. M., 2014, Was the Midcontinent Rift part of a successful seafloor-spreading episode? Geophysical Research Letters, v. 41, p. 1,465–1,470, doi: 10 .1002 /2013GL059176.

Stein, S., Stein, C. A., Elling, R., Kley, J., Keller, G. R., Wysession, M., Rooney, T., Frederiksen, A., and Moucha, R., 2018, Insights from North America's failed Midcontinent Rift into the evolution of continental rifts and passive continental margins: Tectonophysics, v. 744, p. 403–421.

USGS, 2020, GMNA Resources: Geologic Map of North America GIS database: https://ngmdb.usgs.gov/gmna/#gmnaDocs.

Van Schmus, W. R., 1992, Tectonic setting of the Midcontinent Rift System: Tectonophysics, v. 213, no. 1-2, 15 p. https://doi.org/10.1016/0040-1951(92)90247-4.

Van Schmus, W. R., Martin, M. W., Sprowl, D. R., Geissman, J., and Berendsen, P., 1990, Age, Nd and Pb isotopic composition, and magnetic polarity for subsurface samples of the 1100 Ma Midcontinent rift: Geological Society of America Abstracts with Programs, v. 22, no. 7, p. A174.

Woodruff, L. G., Schulz, K. J., Nicholson, S. W., and Dicken, C. L.,2020, Mineral deposits of the Mesoproterozoic Midcontinent Rift System in the Lake Superior region—A space and time classification: Ore Geology Reviews, v. 126, p. 1–21.